Challenging Glass 6 - Conference on Architectural and Structural Applications of Glass
Louter, Bos, Belis, Veer, Nijsse (Eds.), Delft University of Technology, May 2018.

ISBN 978-94-6366-044-0, https://doi.org/10.7480/cgc.6.2172

Thermo-mechanical Investigation of Novel GFRP-glass Sandwich Facade Components

Chiara Bedon [a], Carlos Pascual Agullo [b], Alessandra Luna-Navarro [b], Mauro Overend [b], Fabio Favoino [c]
[a] *University of Trieste, Italy, chiara.bedon@dia.units.it*
[b] *University of Cambridge, United Kingdom, mo318@cam.ac.uk*
[c] *Eckersley O'Callaghan Ltd, United Kingdom*

Modern building envelopes are typically high-technological systems that need to meet strict requirements regarding architectural intent, structural capacity, energy-efficiency and durability. The study presented in this paper is based on recent research performed at the Glass & Façade Technology Research Group (University of Cambridge) that investigates high-performance engineered unitised systems as an alternative to traditional curtain-walls for building facades. The proposed unitised systems has a sandwich design made of two outer glass face sheets separated by, and bonded to, glass fibre-reinforced polymer (GFRP) pultruded profiles. This arrangement results in a lightweight and slim structure that could potentially provide high structural and thermal performances. Results discussed in this paper constitute a preliminary outcome of an extended investigation aimed to assess and compare, by means of Finite Element (FE) numerical simulations, the thermal and structural performances of novel frame-integrated (GFRP-glass) sandwich systems and traditional non-integrated frame curtain wall systems. The reported FE results, as shown, give evidence of the potential of the novel design concept, with improved thermal and structural performances compared to traditional non-integrated systems (up to +10% and +15%, respectively).

Keywords: GFRP-glass sandwich components, Facades, Thermal performance, Mechanical performance, Numerical modelling

1. Introduction

Design of transparent unitised facades (Figure 1) requires a complex multidisciplinary approach that takes into account multiple performance requirements, including structural performance and safety, energy efficiency and occupant comfort, water and air tightness, durability, fire resistance and construction costs (Jin, 2013).

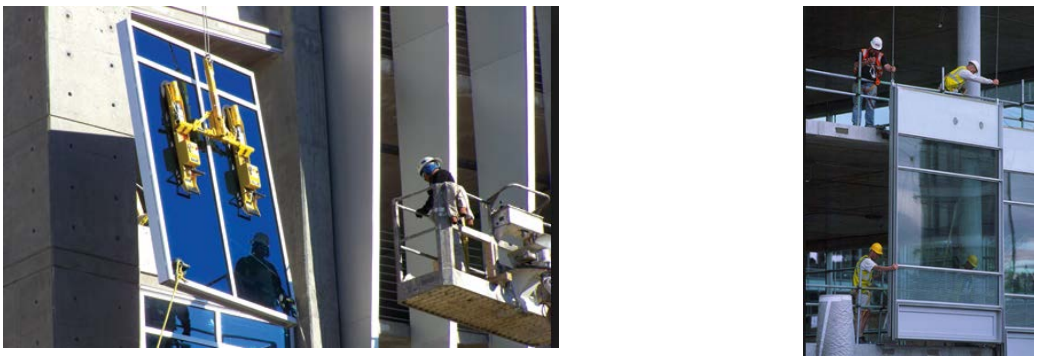

Fig. 1 Installation of traditional non-integrated frame unitised panels for curtain wall systems.

Regulations and design practices encourage the reduction of energy use in buildings, and therefore the reduction of heat transmission losses by minimising the thermal transmittance of the building envelope. Windows and curtain walls can be responsible for a major part of these thermal losses, e.g. by thermally bridging the inside/outside of the building through their highly conductive metallic framing components, Hence, the design of optimized framing components with improved thermal properties can be beneficial to both energy savings and occupant thermal comfort. The use of materials with reduced thermal conductivity, such as plastics or Glass-Fiber Reinforced Polymers (GFRP), can represent a valid alternative to traditional steel or aluminium frames, and can be crafted into various shapes, giving a large freedom of engineering design (Jesus et al., 2013; Cordero, 2015; etc.). Minimising the frame sizes (width and depth) can be beneficial not only in terms of energy efficiency and thermal performance, but can also help in maximising view out and daylight. Such design goals are strictly related to structural requirements for unitised facades, whereas an appropriate choice of materials and dimensions, as well as careful attention for detailing their supports and movement accommodation, is mandatory to ensure appropriate load-bearing performance and deformations of

the so obtained composite assemblies, both at the Ultimate and Service Limit States (Speranzini & Agnetti, 2013; Bedon & Louter, 2018; etc.).

Novel GFRP-glass sandwich panels (Pascual et al., 2017) represent a potential solution to structurally and thermally outperform traditional unitised panels. The GFRP-glass panel investigated by Pascual et al. (2017) was intended to optimize multi-functional aspects in facades, and consisted of two monolithic glass face sheets structurally bonded to GFRP pultruded core profiles (Figure 2). In such a robust and structurally efficient load-bearing component configuration, it was shown that light transmittance can be largely unimpeded and the air cavity between the two glasses can offer potential for high thermal insulation – in this configuration the GFRP component is effectively protected from weathering and acts essentially as a structural spacer between the glass face sheets.

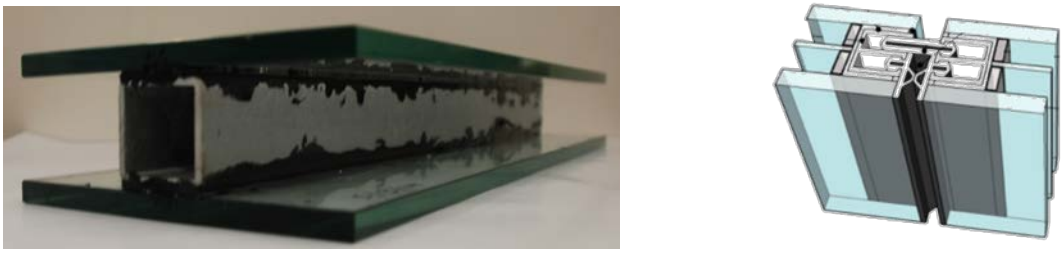

a) b)

Fig. 2 Frame-integrated GFRP-glass sandwich components in a) beam configuration (experimental specimen from (Pascual et al., 2017) and b) unitised panel configuration (schematic view on the connections between two adjacent units from (Cordero, 2015).

Although the energy and structural performances of façades are both fundamental for design, so far these performances have generally been mainly considered as independent aspects. Limited research studies are available in the literature about the interaction between structural and energy efficiency requirements within the design of structural frames of innovative unitised systems. For instance, Zajas & Heiselberg (2014), for example, presented a sensitivity study aimed to assess and optimize the FRP framing geometry for the thermal efficiency of glazing windows. On the other side, several literature documents focus on the structural performance only of glass curtain walls subjected to various mechanical loads, see for example (Behr, 1998; Navar et al. 2013; etc.).

The aim of this paper - derived from an ongoing research collaboration between University of Cambridge (UK) , University of Trieste (IT) and Eckersley O'Callaghan ltd (UK) - is to investigate the basic structural (deflections, stresses and self-weight) and thermal (U-value, ψ-value and condensation risk) properties of GFRP-glass sandwich panels. To this end, preliminary thermal and structural, uncoupled Finite Element (FE) simulations are performed for alternative geometrical and material configurations, in order to assess the potential benefits of this novel sandwich system in comparison to non-integrated, traditional curtain wall systems.

2. Methodology

2.1. Panel configurations

Three glazing panels, all with same plane dimensions (width B=1.5m, height H=3m) and overall dimensions of frame components (50x60 mm approx.), are taken into account in this paper: one frame-integrated GFRP-glass sandwich solution (Figure 3(a)) and two non-integrated GFRP-glass (Figure 3(b)) and aluminium-glass (Figure 3(c)) standard solutions – the latter corresponding to the FW60+ commercial product (Schűco, 2018). A detailed view on the spacer detailing is shown in Figure 3(a), namely consisting of an aluminium tubes with dessicant, primary and secondary adhesive layers (see also (Van Den Bergh et al., 2013)). The reference frame-integrated GFRP-glass solution (Figure 3(a)) comprises:

- Two outer panes: 10-mm thickness monolithic (annealed) glass;
- An inner pane: 5-mm thickness monolithic (annealed) glass;
- An integrated GFRP frame realizing a continuous bracing frame for each modular unit: 50×60×5mm hollow cross-section, namely consisting in two vertical mullions (3m in nominal length) - rigidly connected to the structural background - and two horizontal transoms (1.4m their actual nominal length, being representative of the internal distance between the mullions);
- Adhesive joints bonding the GFRP to the outer glass: 2mm-thickness silicone layers;
- Aluminium spacer tubes with dessicant

The non-integrated GFRP-glass frame solution reported in Figure 3(b) has identical GFRP profile dimensions of the integrated solution, and has a typical triple glazing unit bonded to the frame. Similarly, the reference aluminium-glass panel (Figure 3(c)) is selected for FE comparative purposes since characterized by a structural aluminium frame with essentially the same dimensions of web/flanges than the GFRP-glass panels object of analysis.

At the current stage of the research study, the elastic structural performance of the selected configurations is only investigated. In this regard, the use of annealed, monolithic glass panes in place of pre-stressed and/or laminated glass layers able to offer enhanced pre/post-cracked performances can be rationally justified by the limited magnitude of the assigned external loads. Such an assumption is also in line with equivalent thickness formulations in use for the structural analysis of laminated glass sections, where monolithic plies can be properly taken into account for design purposes (Feldmann et al., 2014). In addition, the thermal performance of the same glass panels is only slightly dependent on their total thickness.

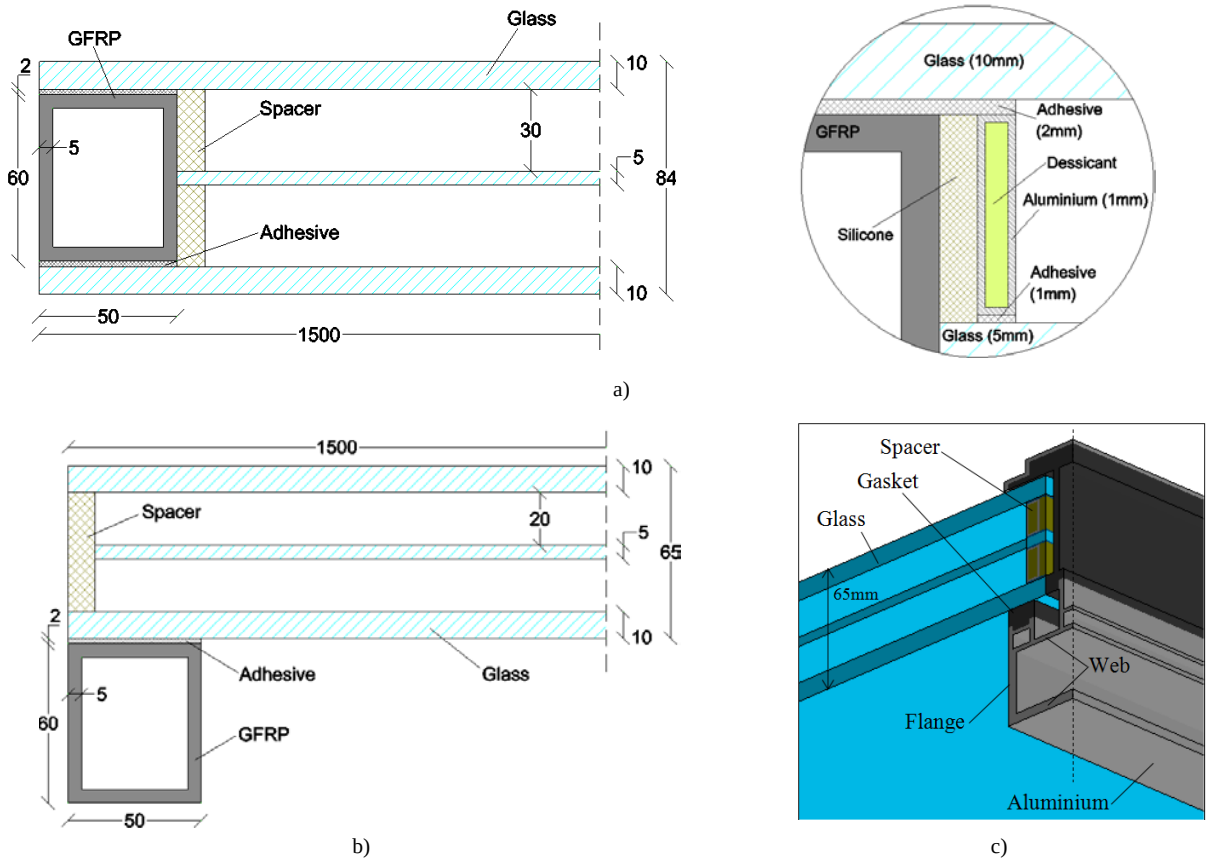

Fig. 3 Sandwich configurations of a) frame-integrated GFRP-glass sandwich panel with detailed view of spacer, b) non-integrated GFRP-glass panel and c) reference non-integrated aluminium-glass panel (all dimensions in mm).

2.2. Control parameters for numerical simulations

The energy and structural performance of the selected systems in Figure 3 are assessed according to specific control parameters, indicated in Table 1. Structural and thermal numerical analyses are hence developed by taking into account specific the loading and boundary conditions described in the following:

Structural performance

- Short-term wind pressure (1kN/m^2)
- Supports at the panel corners (with symmetry boundaries to account for adjacent panels)
- External loads distributed between the three glass panes by accounting for gas cavity (“load sharing”) effects
- Internal (climatic) loads (i.e. temperature variations) are neglected

Thermal performance

- Relative Humidity : 50%
- External condition: T= 0°C, film coefficient= 23 W/m^{2}K
- Internal condition: T= 20°C, film coefficient (glass)= 8.02 W/m^{2}K

The full numerical investigation is carried out in ABAQUS/Standard (Simulia, 2017). Given the selected 1.5m×3m facade modules to investigate (i.e. with cross-sectional features according to Figure 3), two separate FE simulations are implemented to evaluate the thermal and structural performance of each configuration, being the thermal and structural issues related to specific assumptions, such as different loading and boundary conditions. Due to symmetry,

only one quarter of the panel is numerically simulated in both cases, with appropriate constraints. In the following sections, the reference input properties are reported for both of them.

Table 1: Control parameters and input variables for the parametric study

1	CONTROL PARAMETERS	
	STRUCTURAL PERFORMANCE	THERMAL PERFORMANCE
	a) Maximum deflection U_y b) Maximum stress σ in the system components (glass, adhesive, frame) c) Panel weight W	a) Linear heat transfer coefficient ψ □ b) Overall transmittance value U_T c) Transmittance value at the centre of panel U_c c) Surface condensation risk (i.e. lowest indoor temperature)
2	PERFORMANCE ASSESSMENT	
	Best structural & thermal performances, by minimizing the facade assembly thickness	

2.3. Thermal model assumptions

The thermal performance of the facade modules is first assessed by evaluating the U-values (overall and centre of panel values), as well as for the corresponding ψ-values (linear thermal transmittance) and temperature gradient ΔT (for condensation risk assessment).

The thermal boundary conditions reported in Section 2.2, are simulated in accordance with the EN ISO 10077-2:2017 provisions. Typically, thermal simulations are carried out in steady-state heat transfer analyses. The assembled FE model is composed of 8-node brick solid elements (heat transfer elements, DC3D8 type from ABAQUS library). In accordance with the schematic drawings of Figure 3, different solid elements characteristics are used to describe all the module components having different thermal properties, being namely represented by:

- the GFRP or aluminium framing members;
- the outer 10mm thick glass plates;
- the adhesive joints;
- the spacers components (see Figure 3(a)), including dessicant, primary/secondary sealants, aluminium bar detailing;
- the air volumes within the gas cavities;
- the air volumes within the box framing members.

Finally, assuming the modular system being part of a continuous facade, the presence of a linear silicon gasket on the external face of GFRP mullions is also schematized, in accordance with Figure 4(a).

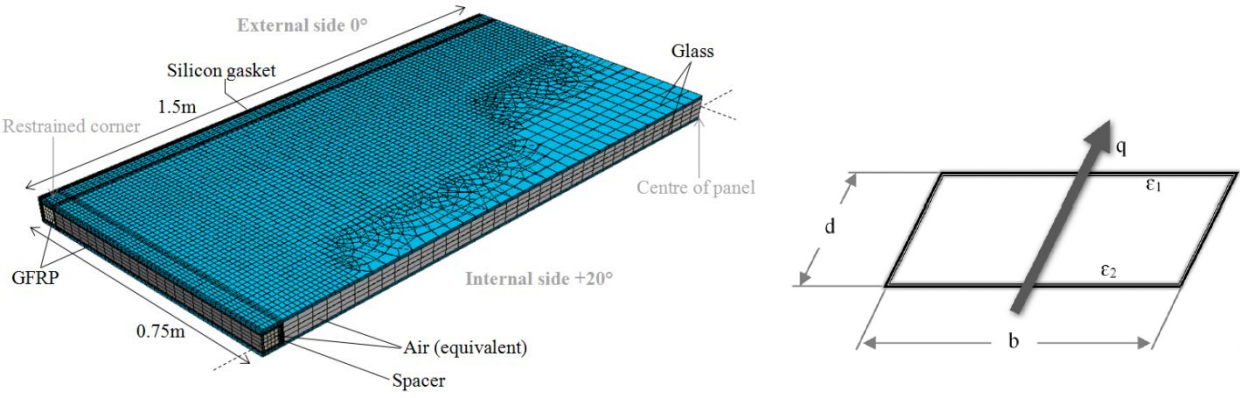

a) b)

Fig. 4a) Typical mesh pattern for the FE thermal model (ABAQUS) and b) reference rectangular cavity for calculation of the equivalent conductivity, in accordance with (Asdrubali et al., 2013).

A free mesh pattern is defined for all the solid components (see an example in Figure 4(a)), so to optimize the computational efficiency of FE simulations, as well as to preserve the accuracy of numerical results, especially close to the panel corners and edges. Following a preliminary sensitivity study, the average mesh size is comprised in the range from 0.2m to 0.0005m, with up ≈150,000 solid elements for one quarter of the facade module.

The thermal characterization of materials is then carried out based on design standards and literature references (EN ISO 10077-2:2017; Asdrubali et al., 2013), see Table 1. Special care is spent for the estimation of the heat transfer within the air volumes enclosed by the glazing cavities and the framing members. To simplify the numerical calculations, both the cavities and the middle glass pane are treated as DC3D8 solid elements, with equivalent thermal conductivity representative of the heat flow by conduction, radiation and convection. In accordance with Figure 4(b) and the EN ISO 10077-2:2017 provisions, an equivalent conductivity λ_{eq} is separately calculated for each one of these volumes, that is:

$$\lambda_{eq} = \frac{d}{R_s} \tag{1}$$

with d [m] denoting the cavity depth, and

$$R_s = \frac{1}{h_a + h_r} \tag{2}$$

In Eq.(2), the h_a and h_r coefficients are able to account for the heat transfer occurring by conduction, convection and radiation inside the cavity where:

$$h_a = \max\left\{\frac{C_1}{d}, C_2 \cdot \Delta T^{1/3}\right\} \tag{3a}$$

$$h_r = 4 \cdot \sigma \cdot T_m^3 \cdot E \cdot F \tag{3b}$$

and C_1=0.025W/mK, C_2=0.73W/m^{2}K$^{4/3}$.

In Eq.(3b), moreover, σ= 5.67×10^{-8}W/m^{2}K^4 is the Stefan-Boltzmann constant; T_m represents the cavity average temperature; E= ((1/ε_1) + (1/ε_2) - 1)$^{-1}$ is the emittance between the involved s_1 and s_2 cavity surfaces (ε_1 and ε_1 their emissivity), F=0.5×(1 + ((1 + (d/b)^2)$^{0.5}$ - (d/b)) is the view factor for rectangular sections, while F=1 is considered for parallel large panes (i.e. glass panes).

Appropriate *surface film* and *surface radiation* thermal interactions are defined on the internal and external surfaces of the outer glass panes, according to the boundary conditions earlier described. The thermal and mechanical properties of the materials and surface interactions are summed up in Table 2. Along the longitudinal and transversal mid-section of the so assembled FE models, finally, symmetry conditions are accounted.

Table 2: Thermal and mechanical material properties for FE modelling (ABAQUS).

* Material properties in use also for the non-integrated module with aluminium frame

					Spacer			
FE model	*Property*	Glass	GFRP	Adhesive	Silicon	Dessicant	Air	Aluminium *
Thermal	Conductivity λ [W/mK]	0.8	0.3	0.3	0.3	0.03	Eq.(1)	240
	Emissivity ε [–]	0.95	/	/	/	/	/	0.8
Structural	Young's modulus E [MPa]	70000	26500 (major) 9900 (minor)	150	/	/	/	70000
	Shear modulus G [MPa]	28455	1900 (major) 3000 (minor)	53.5	/	/	/	26315

According to EN ISO 12631:2017, facade panels can be considered partitioned into several sections using appropriate cut-off planes, which are usually adiabatic boundaries. For the purpose of this study, a quarter of panel is only considered due to symmetry. Although convection within cavities does not follow the symmetrical planes considered in this investigation, given the limited geometrical dimensions of the cavity, the same partition is here considered a valid assumption for FE simulations. In this context, the overall thermal transmittance of the facade element U_T is calculated according to the single assessment method (EN ISO 12631:2017), and then considering the area-weighted

average of all the thermal transmittance of joints and glazing units. According to the single assessment method, the heat flow rate is then derived from numerical modelling of each thermal joint and component. Additionally, the thermal transmittance also evaluated at the centre of panel (U_c), together with the linear heat transfer coefficient ψ (ISO 10077-2).

2.4. Structural model assumptions

The static performance of the above selected facade modules is then investigated. At a preliminary stage of the ongoing research study, the bending performance of the facade systems is assessed under ordinary wind loads. To this aim, compared to section 3.2, appropriate modifications are implemented at the element, boundary and material level. The typical FE model consists in C3D8R solid elements from ABAQUS library. In doing so, the module components having crucial role for the thermal performance assessment, but mostly negligible mechanical contributions, are fully neglected, hence the typical structural FE model consists of:

- the GFRP or aluminium framing members;
- the outer 10mm thick glass panes;
- the middle 5mm thick glass layer;
- the bonding adhesive joints.

In the case of the aluminium curtain wall only (Figure 3(c)), a special attention is spent for the FE description of gaskets and additional details, in accordance with technical drawings (Schűco, 2018).

Linear static simulations are carried out, by progressively increasing the amplitude of a uniform wind pressure (q=1kN/m^2 its nominal value) acting on the external surface of glass. Given the typical installation technique for the examined facade modules, careful consideration is paid for the description of reliable boundary conditions. Assuming symmetry restraints along the middle longitudinal and transversal axes of a given modular unit, the corner supports are supposed to avoid possible U_y displacements as well as rotations around the X and Y axis, see Figure 5. The corner supporting restraints (i.e. rigid brackets, etc.) are mechanically schematized in the form of nodal boundaries for a master RP node lying on the middle axis of mullions' end sections. A kinematic coupling constraint is then established between this RP node and the corresponding end sections of mullions (see the box detail in Figure 5). A rigid mechanical connection is also defined between all the involved structural components of the facade module, in the form of "*tie*" surface constraints enabling possible relative displacements and rotations between the involved surfaces in contact. The same *tie* constraint is used also at the interface between transoms and mullions, hence neglecting possible independent rotations (i.e. close to the panel corners) during the bending stage of the facade module. As also in accordance with preliminary FE studies not included in this paper, the same modelling assumption proved to have negligible effects on the overall bending performance of the examined systems, in particular compared to flexible joints or gaps at the interface between transoms and mullions.

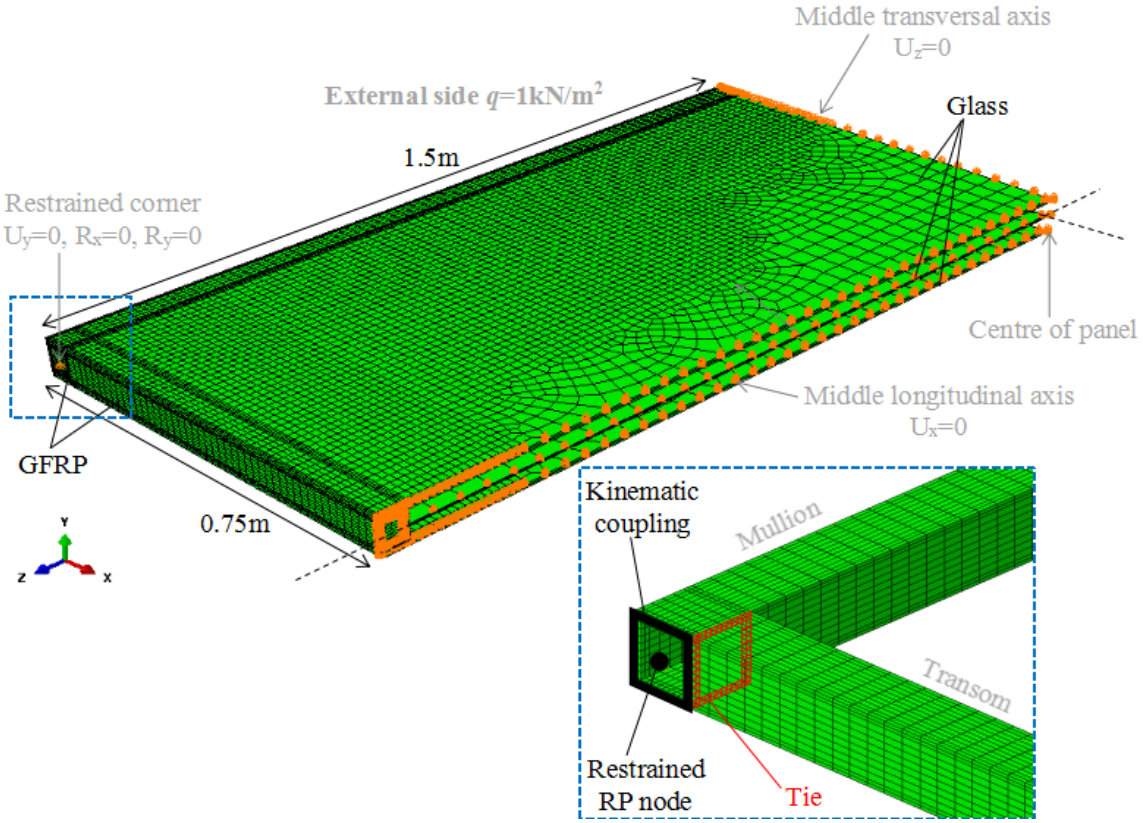

Fig. 5 General features of the typical FE structural model (ABAQUS).

Finally, in accordance with the geometrical assembly reported in Figure 5, the appropriate mechanical interaction between the glass panels in bending are properly taken into account. This includes the potential transmission of the assigned wind pressure q from a glass panel to the others due to the *load sharing* effects. The mechanical "fluid cavity interaction" option from the ABAQUS library is used for each cavity volume since they describe the mechanical behaviour of a fluid (air) within a cavity accordingly to the state equation of ideal gasses. In doing so, a pneumatic gas law with ideal molecular weight M_{air}= 28.97kg/kmol is considered for the air infill, with p_{air}=1atm as reference atmospheric pressure (see also (Bedon & Amadio, 2017)). In this paper, fluid cavity interactions only due to external loads are used for load sharing effects, while possible climatic loads affecting the stress-strain state of the modular components (i.e. pressure, altitude, temperature variations) are fully neglected. In this context, time-loading and temperature effects on the load bearing capacity of the structural components are also disregarded and will be separately assessed in future studies.

Since the imposed external load is of limited magnitude, in addition, the materials are mechanically characterized by the linear elastic constitutive laws, as also reported in Table 2. For the GFRP members only, an orthotropic mechanical model is taken into account (*engineering constants* option from ABAQUS library). Finally, for the reference system in Figure 3(c), the gaskets are described as rubber components (i.e. EPDM type), with a linear elastic behaviour (30MPa their nominal modulus of elasticity, 0.3 the Poisson ratio).

In each simulation, maximum bending deformations and stress peaks are monitored, with careful consideration at selected control points, namely detected at:

- the centre of each glass pane;
- the centre of mullions and transoms;
- the adhesive joints, close to the module corners.

3. Discussion of preliminary FE results

In Figure 6, a selection of FE results is compared for the geometries of interest. The load bearing performance is highlighted by giving evidence of the actual bending stiffness of each system, obtained by comparing the total imposed force with the maximum deflections at the centre of the glass panel exposed to wind pressure. In the same figure, the total U-value (U_T) is also reported for the same modular systems.

As shown, the structural capacities of the glass-GFRP sandwich system are promising, especially in comparison with traditional curtain wall solutions. Maximum deflections of the examined glazing systems - which are only subjected to a limited external pressures - are mostly negligible (≈H/750) with respect to the design provisions (H/60 the allowable deflection at the centre of the panel). Preliminary conclusions on the potential of the GFRP-glass solution can indeed be derived.

Both the bending performances of the sandwich and the layered GFRP-glass systems, for example, show limited stress peaks in the structural components, but marked variations in their overall bending stiffness (in the range of 0.53kN/mm and 0.30kN/mm respectively). The activation of the bending contribution of the outer glass layers, due to the sandwich configuration, results in an overall stiffness up to 1.8 times larger than the layered GFRP section. Minor local bending effects can be also observed for the sandwich system, compared to the layered one (see Figure 7).

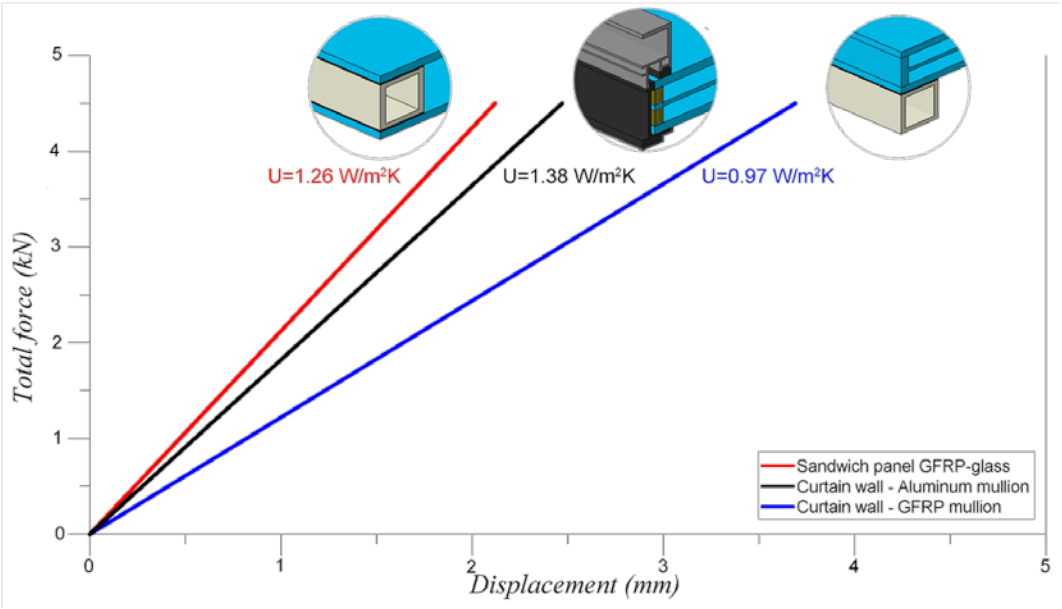

Fig. 6 Force-displacement response of the selected facade systems, including total U-values (ABAQUS).

Figure 6 also compares in terms of bending stiffness the GFRP sandwich system and the non-integrated curtain wall with aluminium framing members. Aluminium frames, being stiffer, can generally minimise the resisting cross-sectional features of a given facade module, with typical thicknesses in the range of 2-4mm (Schűco, 2018). In this study, the bending stiffness of the aluminium system can be estimated in 0.45kN/mm, that is -15% the sandwich module. However, the same FE simulations give also evidence of local buckling phenomena affecting the overall structural performance. In this context, the GFRP sandwich solution proved to offer - even with higher framing thicknesses - stable bending deformations in the range of deflections of interest for this paper, hence suggesting a high structural potential under general design combinations of loads.

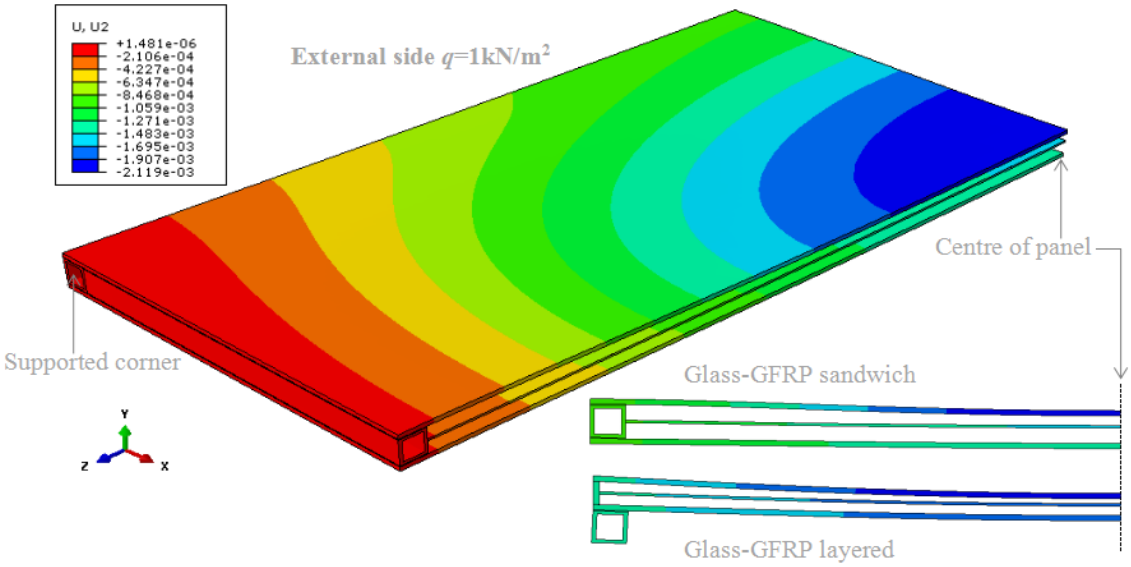

Fig. 7 Bending deformed shape of the sandwich GFRP-glass system, with cross-sectional detail (mid-span), compared to the layered GFRP solution (ABAQUS, legend in [m]).

Worth of interest is then the thermal performance assessment of the explored configurations. As shown in Figure 6, GFRP frames show to be beneficial for the estimated total U-value, due to their typically low thermal conductivity, especially compared to metal frames. The layered GFRP system gives evidence of an enhanced thermal performance, compared to the aluminium curtain wall, but it is able to offer only a limited bending stiffness, compared to the sandwich GFRP-glass system. Table 3, in this regard, reports additional FE results and analyses that provide data for a further feasibility assessment of the explored GFRP-glass system. For instance, the Table 3 indicates that the examined sandwich concept, even with a mostly identical cavity and sealant spacer detailing, offers a safer temperature distribution in terms of condensation risk (see also Figure 8) and suggests the higher potential of the GFRP sandwich solution also in terms of condensation risk.

Table 3: Thermal and mechanical material performances of selected FE models (ABAQUS).

FE model	*Parameter*	GFRP sandwich	GFRP layered	Curtain wall with aluminium frame
Thermal	U_C at the centre of panel [W/m²K]	0.99	0.92	0.98
	U-total U_T [W/m²K]	1.26	0.97	1.38
	Temperature gradient ΔT [°C]	20	20	20
	Minimum surface temperature T_{min} [°C]	15.65	12.63	15.90
	Condensation	No	Yes	No
Structural	Cross-section total thickness [mm]	84 (≈H/35)	125 (≈H/24)	138 (≈H/22)
	Frame weight W [kg] (BxH module)	≈16	≈16	≈20
	Module bending stiffness [kN/mm]	0.53	0.30	0.45

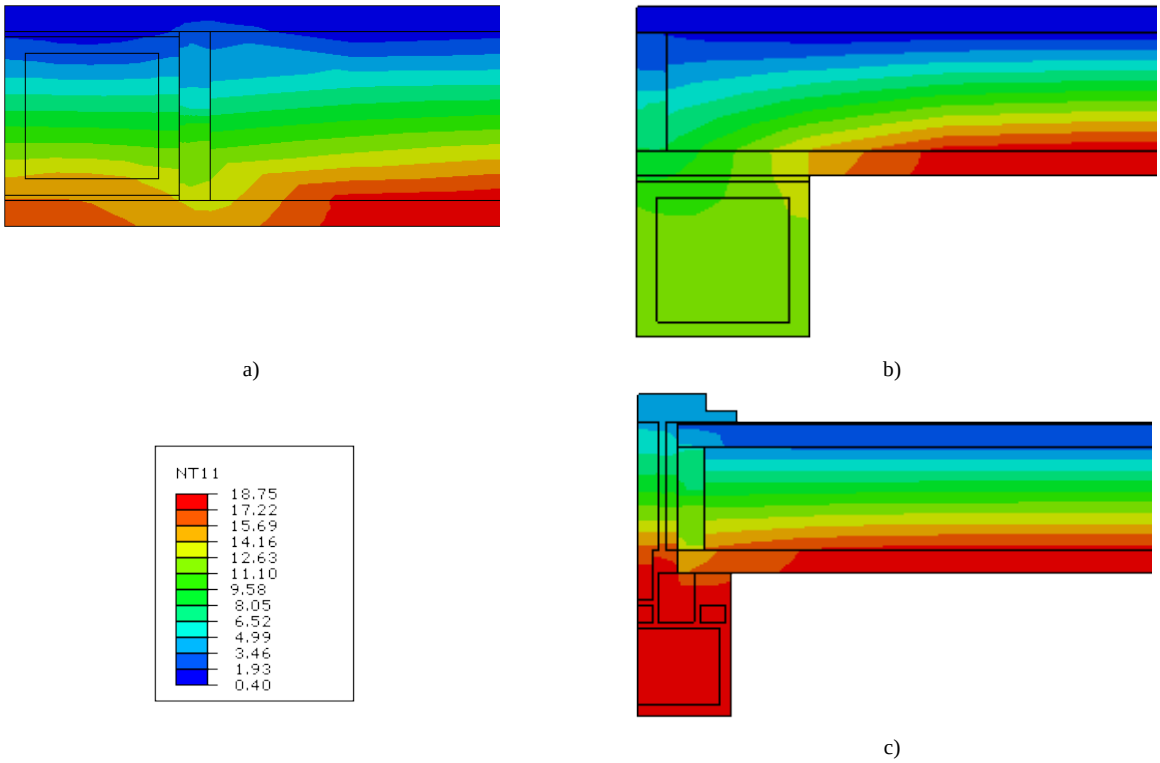

Fig. 8 Cross-sectional detail of temperature distribution (ABAQUS, legend in [°C]), as obtained for the a) GFRP-glass sandwich, b) GFRP-glass layered and c) non-integrated curtain wall with aluminium frame systems.

4. Conclusions and future work

In this paper, a preliminary Finite Element (FE) study on the potential and feasibility of a novel GFRP-glass sandwich facade component was reported, based on thermal and structural numerical simulations with FE analyses. In particular, the GFRP-glass sandwich performance was assessed for comparative purposes to two selected systems, consisting of a traditional aluminium and a non-integrated GFRP-layered curtain wall system. The GFRP-glass sandwich system, as shown, proved to offer enhanced structural performances, compared to the GFRP-layered and aluminium solutions. The traditional metal curtain wall showed similar bending stiffness to the GFRP sandwich panel, but taking advantage of a stiffer, external aluminium frame. In terms of thermal performance, the three compared systems showed also similar results. Further benefits were observed for the GFRP-sandwich solution only, in terms of local temperature distributions, as well as U-total value. Consequently, the thermal efficiency of GFRP members represents an additional key aspect of the novel design concept here presented.

Further extended investigations are required, however. Based on these preliminary FE analysis and comparisons here summarized, further parametric optimization studies are in fact ongoing, aiming to further exploit and optimize the potential of the GFRP-glass sandwich solution from both thermal and structural perspective. As far as even minor geometrical details are in fact expected to modify the overall performance of the examined GFRP-glass sandwich system, variations in the corresponding thermal and mechanical response are expected. The sandwich panel of Figure 3, in this regard, belongs to an extended set of facade modular systems (with up to 400 solutions) that are currently under investigation, being obtained by changing:

- geometrical properties of the GFRP frame members:
  - GFRP section width (40mm, 50mm),
  - GFRP section height (40mm, 50mm, 60mm, 70mm),
  - GFRP section thickness (1/10, 1/15, 1/20 of the maximum section size),
- type of adhesive (structural silicone, acrylate, epoxy),
- adhesive thickness (1mm, 2mm, 3mm),
- spacer details (aluminium bar, steel bar, thermoplastic spacer),

hence leading to extended discussion and comparisons for design optimization.

Acknowledgements

The ongoing COST Action TU1403 “Adaptive Facades Network” (2014-2018, www.tu1403.eu) is gratefully acknowledged for financially supporting a Short-Term Scientific Mission of the first author to University of Cambridge (April 2016), as well as for facilitating networking between the involved researchers.

References

Asdrubali, F., Baldinelli, G., Bianchi, F. (2013). Influence of cavities geometric and emissivity properties on the overall thermal performance of aluminum frames for windows. Energy and Buildings, 60: 298-309

Bedon, C., Amadio, C. (2017). Enhancement of the seismic performance of multi-storey buildings by means of dissipative glazing curtain walls. Engineering Structures, 152: 320-334

Bedon, C., Louter, C. (2018). Numerical investigation on structural glass beams with GFRP-embedded rods, including effects of pre-stress. Composite Structures, 184: 650-661

Behr, R. (1998). Seismic performance of architectural glass in mid-rise curtain wall. Journal of Architectural Engineering, 4(3): 94-98

Cordero, B. (2015). Unitised curtain wall with low thermal transmittance frame integrated within the Insulating Glass Unit through structural adhesives. Ph.D. Dissertation, Polytechnic University of Madrid, free download (last accessed January 2018): http://oa.upm.es/38429/1/BELARMINO_CORDERO_DE_LA_FUENTE.pdf

Correia, J.R., Valarinho, L., Branco, F.A. (2011). Post-cracking strength and ductility of glass-GFRP composite beams. Composite Structures, 93: 2299-2309

EN ISO 10077-2:2017. Thermal performance of windows, doors and shutters - Calculation of thermal transmittance - Numerical methods for frames. CEN, Brussels, Belgium

EN ISO 12631:2017. Thermal performance of curtain walling - Calculation of thermal transmittance. CEN, Brussels, Belgium

Feldmann, M., Kasper, R., Abeln, B., Cruz, P., et al. (2014). Guidance for European Structural design of glass components – support to the implementation, harmonization and further development of the Eurocodes. Report EUR 26439, Joint Research Centre–Institute for the Protection and Security of the Citizen, doi: 10.2788/5523, Pinto Dimova, Denton Feldmann (Eds.)

Jesus M. Cerezo, M., Nunez, M.A. (2015). Fiber Reinforced Polymer (FRP): A New Material Used in Facades of Tall Building. Proceedings of BTBUH 2015 New York Conference, pp. 636-644

Jin, Q. (2013). Towards a whole-life value optimisation model for facade design. Ph.D. Dissertation, University of Cambridge, free download (last accessed January 2018): http://www-g.eng.cam.ac.uk/gft/media/PhD%20Thesis/PhD%20Thesis_Final.pdf

Navar, M, Salim, H., Lusk, B., Perry, K. (2013). Modeling and testing of laminated curtain wall systems under blast loading. Structures Congress 2013, https://doi.org/10.1061/9780784412848.016

Pascual, C., Montali, J., Overend, M. (2017). Adhesively-bonded GFRP-glass sandwich components for structurally efficient glazing applications. Composite Structures, 160: 560-573

Simulia (2017). ABAQUS v. 6.14 computer software and online documentation, Dassault Systems, Providence, RI, USA

Schűco (2018). Schüco Façade FW 60+ - System solutions for vertical facades and skylights, https://www.schueco.com/web2/de-en/architects/products/facades/mullion_transom_facades/schueco_fw_60plus_hi

Speranzini, E., Agnetti, S. (2015). Flexural performance of hybrid beams made of glass and pultruded GFRP. Construction and Building Materials, 94: 249-62

Van Den Bergh, S., Hart, R., Petter Jelle, B., Gustavsen, A. (2013). Window spacers and edge seals in insulating glass units: A state-of-the-art review and future perspectives. Energy and Buildings, 58: 263-280

Zajas, J., Heiselberg, P. (2014). Parametric study and multi objective optimization of window frame geometry. Building Simulation, 7(6): 579-593